

Stability analysis of Wendelstein 7-X configurations with increased mirror ratio

Joachim Geiger

Max-Planck-Institut für Plasmaphysik, IPP-EURATOM Association, Greifswald, Germany

Wendelstein 7-X has been optimized with respect to equilibrium, stability and neoclassical transport properties. The resulting coil system offers a large variety of configurations. The paper summarizes the interchange stability characteristics of the reference configurations and extends them towards configurations with very large toroidal mirror fields. Two classes of configurations are found. In the first one stabilizing properties of shear and magnetic well of the vacuum configurations are decreased, with the effect that extreme cases are found to be Mercier-unstable for all investigated β -values less than 6% with no indication of stabilization by the finite- β magnetic well formation. The second class exhibits a strong additional suppression of the parallel current densities, a factor 3 larger than the reference configurations.

Keywords: stellarator, equilibrium, stability, Wendelstein 7-X, configuration variation

1. Introduction

The magnetic coil system of Wendelstein 7-X is the result of an optimization procedure concerned with the physics properties of a magnetic configuration important for a fusion reactor, such as equilibrium, stability, neoclassical transport and α -particle confinement [1]. The optimization led to the HELICAL-axis-Advanced-Stellarator configuration (HELIASt) with 5 field periods with reduced equilibrium and bootstrap currents. The good α -particle confinement requested a toroidal field mirror of 10% to be present in the configuration which was also beneficial for a further reduction of the bootstrap current. The mirror ratio is defined as $(B(\varphi=0^\circ)-B(\varphi=36^\circ))/(B(\varphi=0^\circ)+B(\varphi=36^\circ))$, where $\varphi=0^\circ$ is the bean-shaped plane in the corners where the toroidal curvature is largest. To avoid major resonances a rather flat profile of the rotational transform ι with a central value above 5/6 and below 1 at the boundary was chosen. A vacuum magnetic well of 1% together with the finite shear in the outer half of the plasma provides stability up to β -values of 5%. For experimental realization, the configuration was cast in a set of 10 modular coils per period for the optimized configuration. To increase the experimental flexibility and to explore the configuration space around the optimization point, the coil currents in the modular coil system can be adjusted independently. Thus, the toroidal field mirror can be varied to influence the size, location and behavior of the trapped particle population. An additional set of 4 planar coils per period, which are slightly inclined, provide the possibility to adjust the rotational transform and the plasma position. A number of reference cases have been proposed already at the beginning of the project [2], with slight modifications later [3],

to show the fundamental flexibility in the value of the rotational transform (low- ι (5/6), standard (5/5), high- ι (5/4)) and its shear (low-shear), the toroidal mirror term (high- (10%) and low-mirror (0%) compared to standard (5%)), the plasma position (in- and outward shifted) and the plasma volume (limiter). Note, that the optimization point in this set is the high-mirror configuration. The standard configuration got its name because it is created by the modular coil system only, with all coils carrying the same current. However, up to now there was no systematic investigation of the large configuration space offered by the W7-X coil system. Only limited work has been done for an ι -variation of the high-mirror case with respect to stability [4], or for neoclassical transport in a more general way for optimized HELIASt-type configurations [5].

This paper starts a broader investigation of the configuration space by investigating the stability behavior of configurations with very large toroidal mirror field. In the beginning the important vacuum field properties of the reference cases are summarized and the implications for interchange stability are shown. Based on these results, the region of the configuration space defined by very large mirror ratios (ca. 20%) is explored with respect to ideal and resistive interchange stability. If not otherwise stated, the pressure profiles used are linear in the normalized toroidal flux s ($p \sim (1-s)$). The free-boundary 3D-equilibria were calculated with VMEC2000 [6]. For the analysis of the local interchange stability, the JMC-code was used [7].

2. Reference cases

The reference cases can be viewed as basic variations of the standard configuration in three directions of the

configuration space: ι , mirror-ratio and plasma position. The low-shear and the limiter case can be interpreted as configurations resulting from combinations of these 3 basic variations. Except for the high- and low- ι cases, all reference cases are located at a boundary- ι value just below the 5/5-resonance. Figs 1 and 2 show shear and vacuum magnetic well depth for the different configurations since these are important quantities in the local interchange stability criteria. It can be seen that the shear increases and the mag-

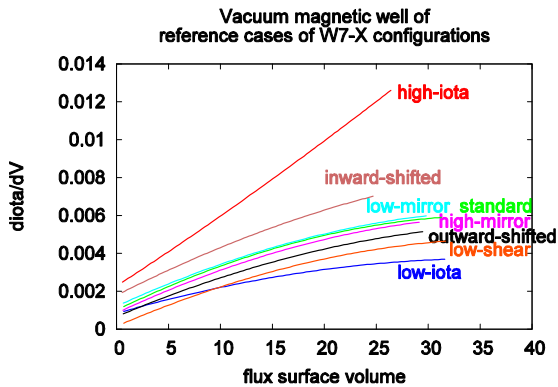


Fig. 1: Shear variation of reference cases.

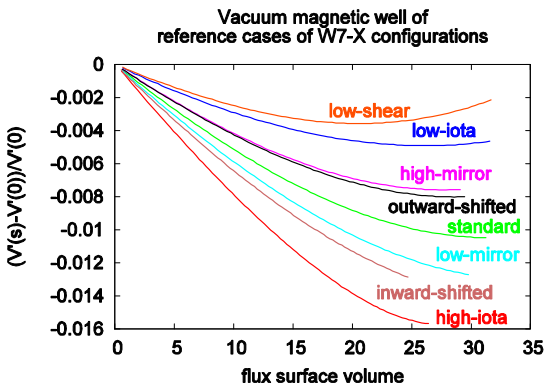


Fig.2: Vacuum magnetic well for reference cases.

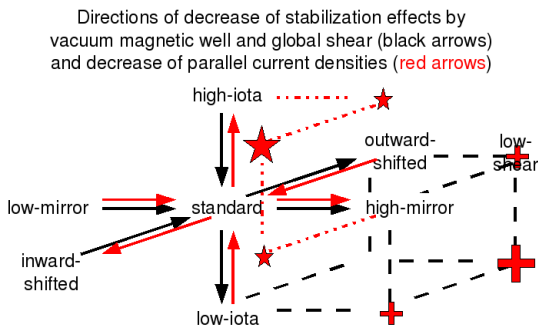


Fig.3: Summary of vacuum configuration changes on shear and magnetic well (black arrows), and on parallel current densities suppression (red arrows). Interesting regions are marked with symbols (stars/crosses).

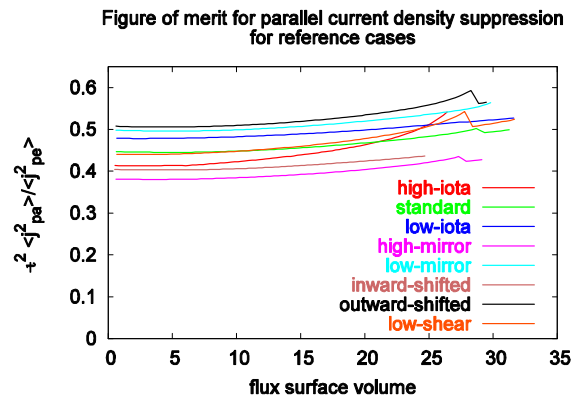


Fig.4: Parallel current density suppression for reference cases. A classical stellarator has the value 2.

netic well deepens with ι , with inward-shifting and with a lower mirror-ratio. Note, that with respect to inward/outward shifting the effect on the magnetic well is opposite to the situation in LHD where outward shifting deepens the magnetic well. For the reference cases, the mirror ratio affects the shear only slightly, but it affects the vacuum magnetic well depth in a way similar to inward/outward shifting. The joint effect can be seen when looking at the profiles of the low-shear configuration which is an outward-shifted configuration with an increased mirror field. This is summarized in Fig.3, where by following the arrows one moves towards configurations less stabilized by shear or vacuum magnetic well.

An analysis with respect to the ideal and resistive interchange criteria show that all configurations except the low-shear configuration are Mercier stable at all investigated $\langle \beta \rangle$ -values (up to 5-6%). The finite shear at outer radii stabilizes the ideal interchange modes in the cases where the derivative of V' is marginal or positive at these radii, e.g. low- ι and high-mirror cases. These show the development of a resistive interchange unstable region at the boundary for already low $\langle \beta \rangle$ -values (below 1%).

Another figure of merit to assess the configuration properties is the ratio of the average of the square of parallel to perpendicular current density (see [7] for its definition). Since the parallel current density is inversely proportional to ι , the dependency can be removed by multiplying the ratio by ι^2 . For a classical stellarator this figure of merit can be estimated to have the value 2. The suppression of the parallel current density by optimization is then obvious by a reduction of the value. Fig. 4 shows that the values for the reference cases are reduced by roughly a factor of 4. Note, that within the reference cases, the ratio falls with increasing ι and mirror-ratio and also with inward-shifting. The latter gives rise to a different behavior than the one observed for shear and vacuum magnetic well.

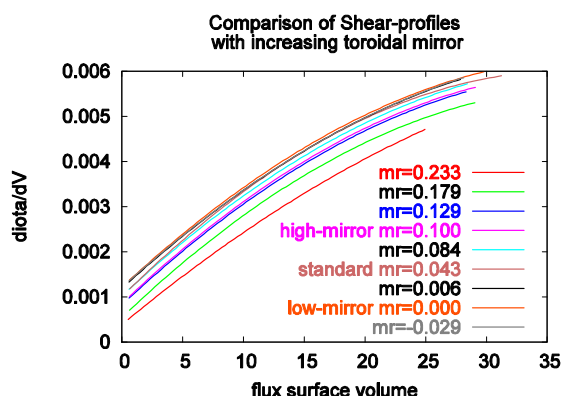


Fig.5: Shear for mirror ratio scan. Reference cases are indicated with names.

3. Cases with very large toroidal mirror

In a first step the mirror ratio was scanned from slightly inverted (ca -3%) to values twice as large as that of the high-mirror reference case (ca 23%) without using the planar coils, thus keeping the boundary value of the rotational transform roughly at 5/5. To perform the scan, the two coil currents around the triangular plane ($\varphi=36^\circ$)

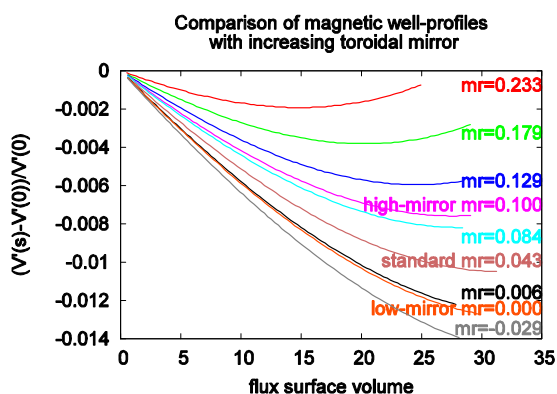


Fig.6: Vacuum magnetic well in mirror scan. Reference cases are indicated with names.

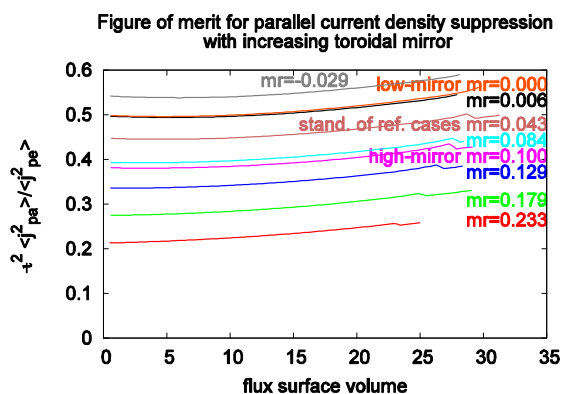


Fig.7: Parallel current density suppression with mirror ratio. Reference cases are indicated with names.

were varied simultaneously while the others were kept constant. The reference cases which vary the toroidal mirror are included in the scan for comparison. The tendency seen with mirror-ratio in the reference cases is obvious: with increasing mirror-ratio, the shear is slightly reduced (Fig.5) and the vacuum magnetic well becomes less stabilizing, so that for the largest mirror ratio considered here, a significant vacuum magnetic hill region exists in the outer half of the configuration (Fig.6). The parallel current densities show a significant suppression with increasing mirror ratio (Fig. 7). For the highest mirror-case (ca 23%), the suppression is almost a factor of 2 larger compared to the high-mirror reference case. The interchange stability behavior is dominated by the reduction of the stabilizing shear and vacuum magnetic well. With increasing mirror ratio the configurations become susceptible to interchange modes in the outer half where, as noted, for the highest mirror ratio a vacuum magnetic hill situation develops. For the latter case, ideal stability is still maintained at very low β -values due to the finite shear, but the outer half becomes unstable to ideal interchange already at moderate $\langle \beta \rangle$ -values of 1%.

In a next step a variation around the configuration

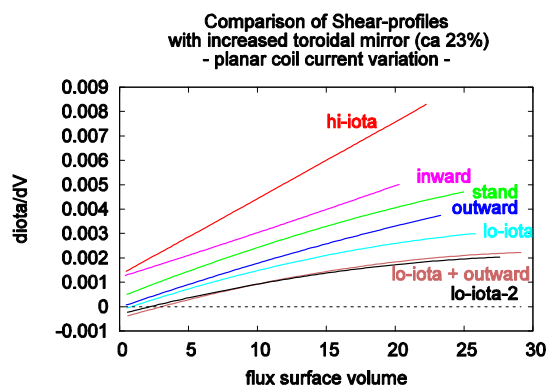


Fig.8: Shear variation with planar coil currents.

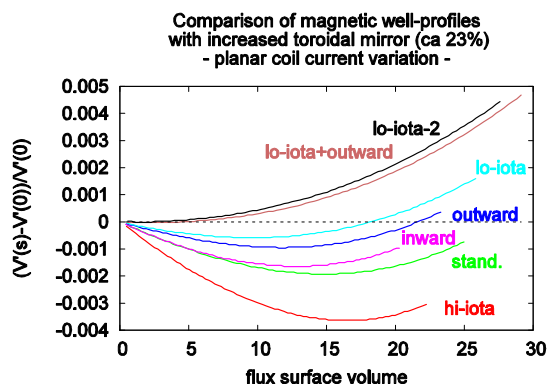


Fig.9: Variation of vacuum magnetic well with planar coil currents.

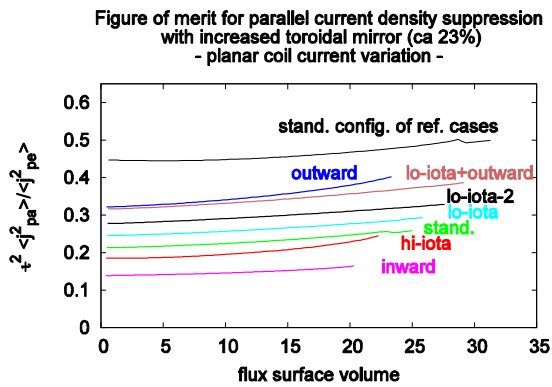


Fig. 10: Parallel current density suppression with planar coil current variation.

with the largest mirror (23%) was performed using the additional planar coils, to investigate the effect of varying ι and the plasma position. The effects seen in Figs 8-10 can be explained from the tendencies discussed previously. The names used for descriptive purposes refer to the center point for the variation, i.e. the case with a mirror ratio of 23%. From the variation two classes of interesting configurations emerge. The most unstable configurations result from going to low ι (lo-iota is around 5/6 and lo-iota-2 is below 5/6) possibly in combination with outward-shifting. In this case, a vacuum magnetic hill region with low shear extends over the entire plasma volume. These configurations are Mercier-unstable from the very beginning with no indication of stabilization with higher β -values. The other class shows a strong suppression of the parallel current density and arises when shifting inward or when going to high- ι . In these configurations, the shear increases and the vacuum magnetic well deepens. The parallel current density is suppressed by an additional factor of 3 compared to the standard configuration of the reference cases. Although these configurations are stable for very low β -values, they develop a Mercier-unstable region at the outer half of the plasma volume which grows as β increases. Not surprisingly, the strong reduction of the parallel current densities leads to very stiff configurations, i.e. very small changes in the ι -profile and the plasma position (Shafranov-shift) with increasing β .

4. Summary and discussion

The configuration space of W7-X is explored for configurations with very large toroidal mirror ratios. The properties of these configurations are the extensions of the properties already found in the reference cases. The exploration led to two configuration classes with large mirror field displaying interesting equilibrium and stability properties.

First, combining low- ι and outward-shifting with large mirror creates configurations with very low shear and a vacuum magnetic hill over the entire plasma cross-section. These configurations are unstable to interchange modes for all β -values. This offers the possibility to investigate the importance of interchange stability in a low-shear device which is expected to behave differently than in large shear devices like LHD. Second, the high- ι , inward-shifted branch of the very large mirror cases reveals configurations with a strong suppression of the parallel current densities. These configurations are less unstable than their low- ι , outward-shifted counterparts. However, they are also unstable from medium $\langle\beta\rangle$ -values onward. Nevertheless, the strong reduction of the parallel current densities leads to rather stiffer configurations with respect to finite- β induced equilibrium changes like the Shafranov-shift.

In a next step, it is planned to extend the analysis to neoclassical transport properties. Due to the large toroidal mirror, particle and energy transport will not be improved with respect to the standard case. However, it is known that the bootstrap current reduces with increasing mirror and may change sign [5]. With respect to neoclassical transport it might be interesting to explore the low or even inverted mirror region of the configuration space in search of configurations being closer to quasi-helical symmetry than the low-mirror configuration.

References

- [1] W. Lotz, J. Nuehrenberg and C. Schwab, *13th Int. Conf. Plasma Physics Control. Nucl. Fus. Res.*, Washington, 1990 (Int. Atomic Energy Agency, Vienna, 1991), Vol. 2, p.603
- [2] J. Kisslinger et al., *Proc. 16th Symp. On Fusion Technology*, London 1990 (North Holland Publ., Amsterdam, 1991), Vol.2, 1520-1524
- [3] T. Andreeva, IPP-Report, IPP III/270 (2002)
- [4] C. Nuehrenberg, *Phys. Plasmas* **3**, 2401 (1996)
- [5] H. Maassberg, W. Lotz and J. Nuehrenberg, *Phys. Fluids B* **5**, 3728-3736 (1993)
- [6] S. Hirshman, W. van Rij and P. Merkel, *Comput. Phys. Comm.* **43**, 143-155 (1986)
- [7] J. Nuehrenberg and R. Zille, in *Theory of Fusion Plasmas Varenna 1987* (Editrice Compositori, Bologna, 1988), Vol. EUR 11336 EN, p.3